Inorg. Chem. **1994**, *33*, 4553–4561

Stabilization of Cobalt Cage Conformers in the Solid State and Solution

Paul V. Bernhardt,[*,1a] **Alexia M. T. Bygott,**[*,1a] **Rodney J. Geue,**[*,1a] **Anthony J. Hendry,**[*,1a]
Bohdan R. Korybut-Daszkiewicz,[*,1a] **Peter A. Lay,**[*,1b] **Jack R. Pladziewicz,**[*,1a,c]
Alan M. Sargeson,[*,1a] **and Anthony C. Willis**[*,1a]

Research School of Chemistry, Australian National University, Canberra, ACT 0200, Australia,
and Inorganic Chemistry Division, School of Chemistry, University of Sydney,
NSW 2006, Australia

Received June 28, 1994[⊗]

The cage complexes $[Co\{(NMe_2)_2sar\}]^{3+}$ and $[Co\{(NMe_2,Me)sar\}]^{3+}$ (sar = sarcophagine = 3,6,10,13,16,19-hexaazabicyclo[6.6.6]icosane; $(NMe_2)_2sar$ = 1,8-bis(dimethylamino)sarcophagine; $(NMe_2,Me)sar$ = 1-(dimethylamino)-8-methylsarcophagine) are obtained by methylation of amino substituents on the parent cage complexes using formaldehyde and formic acid. Further methylation with methyl iodide in dimethyl sulfoxide, or with dimethyl sulfate in *N,N*-dimethylformamide, converts the dimethylamino substituents to trimethylammonium substituents and essentially inverts the circular dichroism (CD) spectrum in comparison to that of the protonated parent cage complex, $[Co\{(NH_3)_2sar\}]^{5+}$. A combination of NMR and electronic spectroscopic measurements indicates that the inversion of the CD spectra is due to conformational inversions in the 1,2-ethanediamine rings from mainly a *lel* conformation in $[Co\{(NH_3)_3sar\}]^{5+}$ to an ob_3 conformation in $[Co\{(NMe_3)_2sar\}]^{5+}$, (without inversion at any of the seven stereogenic centers; Co plus six coordinated amines). This ob_3 conformation was identified in the solid state by an X-ray crystallographic analysis of $[Co\{(NMe_3)_2sar\}](NO_3)_5 \cdot 3H_2O$: monoclinic, $P2_1/n$, $a = 14.382(4)$ Å, $b = 14.604(3)$ Å, $c = 16.998(6)$ Å, $\beta = 100.28(3)°$, $Z = 4$. The electron self-exchange rate constant of the $[Co\{(NMe_3)_2sar\}]^{5+/4+}$ redox couple (+0.05 V vs NHE, 0.011(1) M^{-1} s^{-1} at 25 °C, $I = 0.2$ M (NaCl)) is a factor of 2 smaller than that of the $[Co\{(NH_3)_2sar\}]^{5+/4+}$ couple under the same conditions and is the slowest electron-transfer rate so far measured for a hexaamine cage complex of this type. However, it is still much faster than those of the parent $[Co(en)_3]^{3+/2+}$ and $[Co(NH_3)_6]^{3+/2+}$ couples. This paper also provides hard evidence for the conformations of other Co(III) cage complexes in solution as well as the solid state.

Introduction

The ability of cage ligands like sarcophagine (X_2sar: X = H, Cl, NO_2, NH_3^+, NMe_3^+) to render normally labile oxidation states kinetically inert to ligand exchange has led to many interesting properties and potential applications of these complexes.[2] One of the areas of fundamental interest has been the effect on electron transfer rates brought about by encapsulating the metal ions.[2–17] In particular, the electron self-exchange rate constants for cage complexes are generally much larger than their counterparts with NH_3[18] or 1,2-ethanediamine (en)[19] as ligands. This has been attributed mainly to steric forces which lower the potential energy barrier to electron transfer in the ground electronic states of the cage complexes.[20,21] The molecular mechanics calculations[21,22] that have been used to gauge the rate constant differences for electron transfer between the Co(III/II) redox couples of hexaamine complexes also predict that certain conformational isomers of these cage complexes should have different rate constants of electron self-exchange.

The Co(III/II) redox potentials are also affected by the preferred cavity size of the cage structure.[22,23] With this in mind, conformationally rigid cage complexes were prepared and their electron-transfer properties studied.[13,22,24] The prediction that the cage conformation affects the kinetics and thermodynamics of electron transfer was confirmed from studies of the electron

---

[⊗] Abstract published in *Advance ACS Abstracts,* September 1, 1994.

(1) (a) Australian National University. (b) University of Sydney. (c) On leave from the University of Wisconsin, Eau Claire.

(2) Sargeson, A. M. *Pure Appl. Chem.* **1984**, *56*, 1603–1619, and references therein.

(3) Geue, R. J.; Hambley, T. W.; Harrowfield, J. MacB.; Sargeson, A. M.; Snow, M. R. *J. Am. Chem. Soc.* **1984**, *106*, 5478–5488.

(4) Gahan, L. R.; Hambley, T. W.; Sargeson, A. M.; Snow, M. R. *Inorg. Chem.* **1982**, *21*, 2699–2706.

(5) Creaser, I. I.; Geue, R. J.; Harrowfield, J. MacB.; Herlt, A. J.; Sargeson, A. M.; Snow, M. R.; Springborg, J. *J. Am. Chem. Soc.* **1982**, *104*, 6016–6025.

(6) Bond, A. M.; Lawrance, G. A.; Lay, P. A.; Sargeson, A. M. *Inorg. Chem.* **1983**, *22*, 2010–2021.

(7) Lay, P. A.; Mau, A. W. H.; Sasse, W. H. F.; Creaser, I. I.; Gahan, L. R.; Sargeson, A. M. *Inorg. Chem.* **1983**, *22*, 2347–2349.

(8) Dubs, R. V.; Gahan, L. R.; Sargeson, A. M. *Inorg. Chem.* **1983**, *22*, 2523–2527.

(9) Hammershøi, A.; Sargeson, A. M. *Inorg. Chem.* **1983**, *22*, 3554–3561.

(10) Bakac, A.; Espenson, J. H.; Creaser, I. I.; Sargeson, A. M. *J. Am. Chem. Soc.* **1983**, *105*, 7624–7628.

(11) Creaser, I. I.; Sargeson, A. M.; Zanella, A. W. *Inorg. Chem.* **1983**, *22*, 4022–4029.

(12) Gahan, L. R.; Lawrance, G. A.; Sargeson, A. M. *Inorg. Chem.* **1984**, *23*, 4369–4376.

(13) Geue, R. J.; McCarthy, M. G.; Sargeson, A. M. *J. Am. Chem. Soc.* **1984**, *106*, 8282–8291.

(14) Launikonis, A.; Lay, P. A.; Mau, A. W.-H.; Sargeson, A. M.; Sasse, W. H. F. *Sci. Pap. Inst. Phys. Chem. Res.* (*Jpn.*) **1984**, *78*, 198–205.

(15) Creaser, I. I.; Gahan, L. R.; Geue, R. J.; Launikonis, A.; Lay, P. A.; Lydon, J. D.; McCarthy, M. G.; Mau, A. W.-H.; Sargeson, A. M.; Sasse, W. H. F. *Inorg. Chem.* **1985**, *24*, 2671–2680.

(16) Bernhard, P.; Sargeson, A. M. *Inorg. Chem.* **1987**, *26*, 4122–4125.

(17) Bernhard, P.; Sargeson, A. M. *J. Am. Chem. Soc.* **1989**, *111*, 597–606.

(18) Geselowitz, D.; Taube, H. *Adv. Inorg. Bioinorg. Mech.* **1982**, *1*, 391–407; Hammershøi, A.; Geselowitz, D.; Taube, H. *Inorg. Chem.* **1984**, *23*, 979–982.

(19) Dwyer, F. P.; Sargeson, A. M. *J. Phys. Chem.* **1961**, *65*, 1892–1894.

(20) Geselowitz, D. *Inorg. Chem.* **1981**, *20*, 4457–4459.

(21) Geue, R. J.; Pizer, R.; Sargeson, A. M. *Abstracts of Papers*; 183rd National Meeting of the American Chemical Society; Las Vegas, NV, Apr 1982; American Chemical Society: Washington DC, 1982; INOR 62; Geue, R. J.; Sargeson, A. M. To be submitted for publication.

(22) Hendry, A. J. Ph.D. Thesis, Australian National University, 1986; Geue, R. J.; Hendry, A. J.; Sargeson, A. M. *J. Chem. Soc., Chem. Commun.* **1989**, 1646–1647.

(23) Hambley, T. W. *Inorg. Chem.* **1988**, *27*, 2498–2501.

(24) Hendry, A. J.; Naidoo, K. J.; Thornton, D. A. *J. Chem. Soc., Chem. Commun.* **1989**, 998–1000.

0020-1669/94/1333-4553$04.50/0

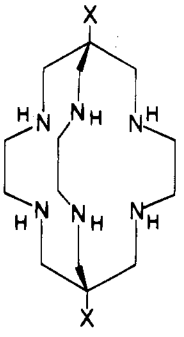

sar (X = H)

transfer properties of the conformationally stable *lel*$_3$ and *ob*$_3$ isomers of the $[Co\{(NH_3)_2Me_3sar\}]^{5+/4+}$ ions prepared from $[Co(pn)_3]^{3+}$ (pn = 1, 2-propanediamine).[22] The *lel* and *ob* nomenclature refers to the orientation of the C—C bond, within the five-membered chelate ring defined by the 1,2-ethanediamine fragments, relative to the C_3 axis of the complex ion, i.e. parallel or oblique. The Λ-*lel*$_3$ and Λ-*ob*$_3$ conformers of this complex also exhibit interesting circular dichroism (CD) spectra that are essentially inverted with respect to each other for the same absolute configuration about the metal ion. The two conformers also differ markedly in their electrochemical and other spectroscopic properties.[22]

In the course of examining substituent effects on the Co(III/II) redox couples of sar cage complexes, it was found that those with dimethylammonium and trimethylammonium substituents in the apical positions[6,25,26] exhibited anomalous spectroscopic properties compared with other cage complexes. These details are reported here along with their rationalization in terms of the conformational structures of the encapsulated ions in solution and in the solid state.

Experimental Section

Instrumentation. Absorption spectra were recorded using Cary 14 or 118C spectrophotometers. Optical rotary dispersion (ORD) and circular dichroism (CD) experiments were performed with a Perkin-Elmer P22 spectropolarimeter and a Cary-60 CD spectropolarimeter, respectively, using solution concentrations of ~1.6 mM. Molar absorption coefficients (ϵ) are quoted in M^{-1} cm^{-1} and molecular rotations $(M)_D$ in deg M^{-1} m^{-1}, for the sodium D line (589 nm), unless otherwise stipulated. ^1H NMR spectra were recorded with a Jeol 100 MHz Minimar spectrometer using NaTPS (sodium (trimethylsilyl)-propanesulfonate) as an internal standard. ^{13}C NMR spectra were obtained using a JNM-FX 60 Fourier transform spectrometer with 1,4-dioxane as internal standard. The 300 MHz ^1H and 75.9 MHz ^{13}C and 2D NMR spectra were recorded with a Varian VXR-300 Fourier transform NMR spectrometer. Chemical shifts (δ) are expressed in ppm as positive downfield shifts from 1,4-dioxane (^{13}C: 67.39 ppm vs TMS) or NaTPS (^1H). Infrared spectra were recorded from KBr disks with Perkin-Elmer 457 or 683 infrared spectrometers. Evaporations were performed at reduced pressures (~20 Torr) and in a water bath at ~50 °C using a Büchi rotary evaporator. Standard electrochemical measurements were performed using either a PAR Model 174A polarographic analyzer coupled with a Houston Instrument Omnigraphic 2000 recorder, a PAR Model 170 electrochemistry system, or a BAS 100 electrochemical analyzer. In all cases, a three electrode system was used with full iR compensation. The auxiliary electrode consisted of a Pt wire and the reference electrode was either $Hg/Hg_2Cl_2/KCl$(saturate) (SCE) or Ag/AgCl/KCl(saturate). The mercury working electrodes used were a PAR Model 172A DME, a PAR Model 303 static mercury drop electrode (SMDE), or a hanging mercury drop electrode (HMDE). Pt and Au working electrodes were either wires or Beckman rotating electrodes. All solutions were degassed with Ar.

Syntheses. All chemicals used were AR grade. $[Co\{(NH_3)_2sar\}]Cl_5 \cdot 1.5H_2O$, Δ-(+)$_D$-$[Co\{(NH_3)_2sar\}]Cl_5 \cdot H_2O$, Λ-(−)$_D$-$[Co\{(NH_3)_2sar\}]Cl_5 \cdot H_2O$, and $[Co\{(NH_3,Me)sar\}]Cl_4$ were synthesized by literature methods,[3] from (±)-$[Co(en)_3]Cl_3$, Δ-(−)$_D$-$[Co(en)_3]Cl_3$, Λ-(+)$_D$-$[Co(en)_3]Cl_3$, and $[Co(sen)]Cl_3$ respectively.

(1,8-Bis(dimethylammonio)-3,6,10,13,16,19-hexaazabicyclo[6.6.6]icosane)cobalt(III) Chloride Pentahydrate, $[Co\{(NHMe_2)_2sar\}]Cl_5 \cdot 5H_2O$. Method 1. $[Co\{(NH_3)_2sar\}]Cl_5 \cdot 1.5H_2O$ (8.3 g, 0.0015 mol) was refluxed for 48 h in a mixture of 98% formic acid (80 mL) and 30% formaldehyde (30 mL). The mixture was evaporated to dryness on a rotary evaporator, and the residue was crystallized from 1 M HCl by the slow addition of ethanol. The orange crystals were filtered and dried under vacuum. Yield: 9.0 g (90%). Anal. Calcd for $C_{18}H_{44}N_8Cl_5Co \cdot 5H_2O$: C, 30.94; H, 7.79; N, 16.03; Co, 8.43; Cl, 25.36. Found: C, 30.9; H, 8.0; N, 16.0; Co, 8.9; Cl, 25.4. ^1H NMR (300 MHz, DCl/D_2O): 3.37, 3.57 (AB doublet of doublets, 12H, $J_{12} = -13$ Hz, CH_2 caps); 3.13, 3.88 (AA′BB′ coupling pattern, 12H, CH_2 en); 3.02 (s, 12H, $NH(CH_3)_2$); (300 MHz, D_2O/py): 2.89, 3.19 (AB doublet of doublets, 12H, $J_{12} = -14$ Hz, CH_2 caps); 2.98, 3.67 (AA′BB′ coupling pattern, 12H, CH_2 en); 2.30 (s, 12H, $N(CH_3)_2$); (100 MHz, 36% DCl/D_2O): 6.99 (s, 6H, coordinated NH); 2.6−4.5 (complex coupling pattern, 24H, CH_2); 3.05 (s, 12H, $NH(CH_3)_2$).

The same procedure was used for the synthesis of the chiral complexes except optically pure forms of $[Co\{(NH_3)_2sar\}]^{5+}$ were used. Anal. Calcd for $C_{18}H_{44}N_8Cl_5Co \cdot 5H_2O$ for the product from the Λ-(−)$_D$-$[Co\{(NH_3)_2sar\}]^{5+}$ isomer: C, 30.94; H, 7.79; N, 15.63. Found: C, 30.6; H, 8.0; N, 15.95. Anal. Calcd for $C_{18}H_{44}N_8Cl_5Co \cdot 6H_2O$ for the product from the Δ-(+)$_D$-$[Co\{(NH_3)_2sar\}]^{5+}$ isomer: C, 30.16; H, 7.87; N, 15.63. Found: C, 30.0; H, 7.7; N, 15.5.

(1,8-Bis(dimethylammonio)-3,6,10,13,16,19-hexaazabicyclo[6.6.6]icosane)cobalt(III) Chloride Tetrahydrate, $[Co\{(NHMe_2)_2sar\}]Cl_5 \cdot 4H_2O$, and (1-(Dimethylammonio)-8-methyl-3,6,10,13,16,19-hexaazabicyclo[6.6.6]icosane)cobalt(III) Chloride Dihydrate, $[Co\{(NHMe_2,Me)sar\}]Cl_4 \cdot 2H_2O$. Method 2. $[Co\{(NH_3)_2sar\}]Cl_5 \cdot 1.5H_2O$ or $[Co\{(NH_3,Me)sar\}]Cl_4 \cdot H_2O$ (0.0024 mol) was converted to the acetate salt by using a column of the acetate form of Dowex 1-X8 anion exchange resin. The eluate was evaporated to dryness and dissolved in acetonitrile (60 mL). To the solution was added 38% aqueous HCHO (15 g, 0.10 mol) and glacial acetic acid (5 mL), and the solution was stirred rapidly while $NaNCBH_3$ (1.5 g, 0.015 mol) was added. After the solution was left overnight, it was diluted with water (500 mL) and sorbed on a column (4.5 cm × 6 cm) of Dowex 50W-X2 cation exchange resin (H^+-form). The column was washed with water (1.5 L) and 0.5 M HCl (500 mL) and the complex was eluted with 3 M HCl. *Caution! These manipulations should be performed in a well-ventilated fume hood because of the presence of CN^- in the reaction mixture after the hydrolysis of $NCBH_3^-$.* The eluate was evaporated until crystallization commenced. Ethanol (~3 volumes) was added and the mixture heated and allowed to cool to room temperature. The solution was cooled further in an ice bath (2 h). The yellow crystals of $[Co\{(NHMe_2)_2sar\}]Cl_5 \cdot 4H_2O$ or $[Co\{(NHMe_2,Me)sar\}]Cl_4 \cdot 2H_2O$ were collected, washed with EtOH and diethyl ether, and dried *in vacuo* over P_4O_{10}. Both complexes were obtained in yields of >90%. $[Co\{(NHMe_2)_2sar\}]Cl_5 \cdot 4H_2O$ had properties identical to those of a sample obtained by method 1. Data for $[Co\{NHMe_2,Me)sar\}]Cl_4 \cdot 2H_2O$ are as follows. Anal. Calcd for $C_{17}H_{40}N_7Cl_4Co \cdot 2H_2O$: C, 35.24; H, 7.66; N, 16.93; Co, 10.17; Cl, 24.48. Found: C, 35.3; H, 8.2; N, 16.9; Co, 10.2; Cl, 24.6. ^1H NMR (100 MHz, D_2O/pD 7): 2.8−4.0 (complex coupling pattern, 24H, CH_2); 2.98 (s, 6H, $N(CH_3)_2$); 0.98 (s, 3H, CH_3).

Λ-(+)$_D$-$[Co\{(NHMe_2)_2sar\}]Cl_5 \cdot 4H_2O$ and Δ-(−)$_D$-$[Co\{(NHMe_2)_2sar\}]Cl_5 \cdot 4H_2O$ were prepared by essentially the same procedure from Λ-(−)$_D$-$[Co\{(NH_3)_2sar\}]Cl_5$ and Δ-(+)$_D$-$[Co\{(NH_3)_2sar\}]Cl_5$, respectively. Anal. Calcd for $C_{18}H_{44}N_8Cl_5Co \cdot 4H_2O$: C, 31.75; H, 7.70; N, 16.53; Co, 8.66; Cl, 26.04. Found: C, 31.8; H, 7.1; N, 16.5; Co, 8.5; Cl, 26.3.

Partial methylations were achieved by adding smaller amounts of $NaNCBH_3$ and HCHO during the reductions. However, separations of the various products from $[Co\{(NH_3)_2sar\}]^{5+}$ reactions on SP-Sephadex C-25 with NaCl, Na_2(+)$_D$-tartrate, and/or $(NH_4)_2CO_3$, as

---

(25) Lay, P. A., Ph.D. Thesis, Australian National University, 1981; Chapters 2 and 4.

(26) Lawrance, G. A.; Lay, P. A.; Sargeson, A. M. *Inorg. Chem.* **1990**, *29*, 4808−4816.

eluants, proved to be difficult and only incomplete separations were obtained. In addition to the product characterized above, the partially-methylated product, $[Co\{(NHMe_2,NH_2Me)sar\}]^{5+}$, was identified by ^1H-decoupled ^{13}C NMR spectroscopy after chromatographic separations. This complex and other partially-methylated complexes were not isolated in sufficient amounts for complete characterization.

(1,8-Bis(dimethylamino)-3,6,10,13,16,19-hexaazabicyclo[6.6.6]-icosane)cobalt(III) Trifluoromethanesulfonate Monohydrate, $[Co\{(NMe_2)_2sar\}](CF_3SO_3)_3\cdot H_2O$. $[Co\{(NHMe_2)_2sar\}]Cl_5\cdot 4H_2O$ (6.7 g, 0.001 mol) was dissolved in trifluoromethanesulfonic acid (6 mL), and the HCl that evolved was removed under reduced pressure at 70 °C for 5 h. After the mixture was cooled, diethyl ether (200 mL) was added cautiously to the solution. The resulting yellow precipitate was filtered, washed with diethyl ether, and recrystallized from water/ethanol solution. Yield: 8.1 g (90%). Anal. Calcd for $C_{21}H_{42}N_8F_9S_3O_9$-$Co\cdot H_2O$: C 28.18; H, 4.95; N, 12.52. Found: C, 28.26; H, 5.10; N, 12.90.

(1,8-Bis(trimethylammonio)-3,6,10,13,16,19-hexaazabicyclo[6.6.6]-icosane)cobalt(III) chloride hexahydrate, $[Co\{(NMe_3)_2sar\}]Cl_5\cdot 6H_2O$. Method 1. $[Co\{(NMe_2)_2sar\}](CF_3SO_3)_3\cdot 3H_2O$ (3 g, 0.003 mol), dimethyl sulfate (3 mL), and sodium carbonate (0.4 g) were stirred in *N*,*N*-dimethylformamide (50 mL) for 24 h. The reaction mixture was diluted with water (200 mL) and absorbed onto a Dowex 50W-X2 column. After the column was washed with 1 M HCl, the complex was eluted with 3 M HCl. The eluate was evaporated to dryness under reduced pressure, and the residue was recrystallized from water/ethanol solution. The yellow crystals were filtered off and dried under vacuum. Yield: 2.2 g (88%). Anal. Calcd for $C_{20}H_{48}N_8CoCl_5\cdot 6H_2O$: C, 32.25; H, 8.12; N, 15.04; Cl, 23.80. Found: C, 31.9; H, 8.5; N, 14.9; Cl, 24.4. ^1H NMR (300 MHz, D_2O): 3.43, 3.75 (AB doublet of doublets, 12H, $J_{12} = -13$ Hz, CH_2 caps); 3.16, 3.89 (AA′BB′ coupling pattern, 12H, CH_2 en); 3.29 (s, 1 8H, $N(CH_3)_2$). ^1H NMR (100 MHz, DCl/D_2O): 7.07 (s, 6H, NH) 2−4 (complex coupling pattern, 24H, CH_2); 3.3 (s, 18H, $N(CH_3)_3$).

The enantiomers were prepared in an identical manner from the chiral $[Co\{(NHMe_2)_2sar\}]^{5+}$ complexes except that they were purified by chromatography on a column of SP-Sephadex C25 using 0.2 M Na_2-$(+)_D$-tartrate as the eluant. Anal. Calcd for Δ-$(-)_D$-$C_{20}H_{48}N_8$-$CoCl_5\cdot 7H_2O$ obtained from the Δ-$(+)_D$-$[Co\{(NH_3)_2sar\}]^{5+}$ precursor: C, 31.49; H, 8.19; N, 14.69. Found: C, 31.2; H, 8.3; N, 14.9. $[M]_D = -2300$ deg M^{-1} m^{-1}. Anal. Calcd for Λ-$(+)_D$-$C_{20}H_{48}N_8CoCl_5\cdot 7H_2O$ obtained from the Λ-$(-)_D$-$[Co\{(NH_3)_2sar\}]^{5+}$ precursor: C, 31.49; H, 8.19; N, 14.69. Found: C, 31.4; H, 8.3; N, 14.9. $[M]_D = +2240$ deg M^{-1} m^{-1}.

(1,8-Bis(trimethylammonio)-3,6,10,13,16,19-hexaazabicyclo[6.6.6]-icosane)cobalt(III) Chloride Hexahydrate, $[Co\{(NMe_3)_2sar\}]Cl_5\cdot 6H_2O$, and (1-(trimethylammonio)-8-methyl-3,6,10,13,16,19-hexaazabicyclo-[6.6.6]icosane)cobalt(III) Chloride Tetrahydrate, $[Co\{(NMe_3,Me)sar\}]Cl_4\cdot 4H_2O$. Method 2. $[Co\{(NHMe_2)_2sar\}]Cl_5\cdot 4H_2O$ (0.30 g) was dissolved in water, and Dowex 1-X8 resin (acetate form, 10 g dry weight) was added. The solution was stirred at ~25 °C for 30 min and filtered. The resin was washed with water (2 × 10 mL) and the combined filtrates were evaporated to dryness. The solid was dissolved in DMSO (200 mL), and CH_3I (2 mL) was added. After the mixture was stirred for 24 h at ~25 °C, the resulting solution was diluted with water (2 L) and sorbed onto a short column (7 × 2 cm) of Dowex 50W-X2 resin. The column was washed with water (500 mL) and 1 M HCl (500 mL), and the complex was eluted with 4 M HCl. Evaporation of the eluate to dryness yielded a yellow solid which was recrystallized from hot water (15 mL) and 12 M HCl (2.5 mL) by the addition of ethanol (~10 mL) until the solution was turbid, followed by slow cooling. Yield: 95%.

Λ-$(+)_D$-$[Co\{(NMe_3)_2sar\}]Cl_5\cdot 6H_2O$ (Anal. Calcd for $C_{20}H_{48}N_8Co$-$Cl_5\cdot 6H_2O$: C, 32.25; H, 8.12; N, 15.04. Found: C, 32.3; H, 7.9; N, 14.9). Δ-$(-)_D$-$[Co\{(NMe_3)_2sar\}]Cl_5\cdot 6H_2O$, and $[Co\{(NMe_3,Me)sar\}]$-$Cl_4\cdot 4H_2O$ were prepared by essentially the same procedure from Λ-$(+)_D$-$[Co\{(NHMe_2)_2sar\}]Cl_5\cdot 4H_2O$, Δ-$(-)_D$-$[Co\{(NHMe_2)_2sar\}]Cl_5\cdot 4H_2O$ and $[Co\{(NHMe_2,Me)sar\}]Cl_4\cdot 2H_2O$, respectively.

(1,8-Bis(trimethylammonio)-3,6,10,13,16,19-hexaazabicyclo[6.6.6]-icosane)cobalt(III) Nitrate Trihydrate, $[Co\{(NMe_3)_2sar\}](NO_3)_5\cdot 3H_2O$. To a solution of $[Co\{(NMe_3)_2sar\}]Cl_5\cdot 6H_2O$ (0.300 g, 0.40 mmol) in water (30 mL) was added $AgNO_3$ (0.342 g, 2.0 mmol) with stirring. The resulting suspension was gravity filtered. Yellow crystals of the nitrate salt, suitable for X-ray analysis, formed by slow evaporation of the filtrate at ~25 °C. These were collected by filtration and washed with ethanol. Anal. Calcd for $C_{20}H_{48}N_{13}CoO_{15}\cdot 3H_2O$: C, 29.16; H, 6.85; N, 22.11. Found: C, 29.03; H, 6.51; N, 21.84.

(1,8-Bis(trimethylammonio)-3,6,10,13,16,19-hexaazabicyclo[6.6.6]-icosane)cobalt(II) Tetrachlorozincate, $[Co\{(NMe_3)_2sar\}](ZnCl_4)_2$. This was prepared by Zn/Hg reduction of an aqueous solution of $[Co\{(NMe_3)_2sar\}]Cl_5\cdot 6H_2O$ under a nitrogen atmosphere and subsequent precipitation of the tetrachlorozincate complex. Anal. Calcd for $C_{20}H_{48}N_8Cl_8CoZn_2$: C, 27.49; H, 5.54; N, 12.82. Found: C, 27.45; H, 6.4; N, 12.71.

Kinetics Experiments. Solutions of $(+)_D$- and $(-)_D$-$[Co\{(NMe_3)_2sar\}]Cl_5\cdot 6H_2O$ (~5×10^{-3} M in 0.2 M NaCl) were thoroughly deoxygenated with O_2-free dinitrogen, and one isomer was reduced with granulated Zn/Hg over a period of 16 h. Equal volumes of the solutions were mixed in a 2-cm ORD cell (temperature controlled at 25.0 ± 0.1 °C) using a stopped-flow apparatus[27] that had also been flushed with O_2-free dinitrogen. The electron-transfer reactions were followed by racemization of the mixture ($\Delta\alpha$ ~0.4°) using a Perkin-Elmer P22 polarimeter at 468 nm (the wavelength for maximum rotational change). At this wavelength, most of the rotation was contributed by the Co(III) ion ([M] ~ 9000 deg M^{-1} m^{-1}) and little by the Co(II) ion ([M] ~ 500 deg M^{-1} m^{-1}). Two experiments gave self-exchange rate constants of 0.012 and 0.0091 M^{-1} s^{-1} at $I = 0.2$ M. At $I = 1.0$ M (NaCl), the rate constants were 0.013 and 0.015 M^{-1} s^{-1}.

X-ray Crystal Structure Analysis. A yellow hexagonal needle of $[Co\{(NMe_3)_2sar\}](NO_3)_5\cdot 3H_2O$ was coated with a thin layer of epoxy resin and mounted on a Rigaku AFC-6S diffractometer equipped with a graphite monochromator. Using molybdenum radiation, 20 reflections were located and indexed on a monoclinic cell, and Laue $2/m$ symmetry was confirmed. Lattice parameters were determined by least-squares analysis of the setting angles of 25 reflections $11 < 2\theta < 18°$ (λ (Mo Kα) = 0.710 73 Å). Crystallographic data are given in Table 1. Intensity data for reflections $h,k,\pm l$ (h, 0 to 17; k, 0 to 17, l, −20 to +19) were collected using $\omega - 2\theta$ scans of width $(1.1 + 0.34 \tan \theta)°$ in ω at a rate of 2° min^{-1} in ω (weak reflections were measured with up to four scans) with background counts for one-fourth of the scan time on each side of every scan. Three standards measured at intervals of 150 reflections showed no significant decrease in intensity during data collection. Data were corrected for absorption (transmission range 0.942−0.958).

The non-hydrogen atoms were located by Patterson and difference-Fourier techniques. When anisotropic displacement factors were employed for the non-hydrogen atoms, it was observed that the displacement factors for the oxygen atoms of nitrate 5 were extremely large. Examination of the electron density in this region of the cell suggested that there were two orientations for the nitrate anion, depending on the occurrence of the partially occupied water site O(3). Two nitrate frameworks of occupancies p and $1 - p$, respectively, were set up to mimic the electron density, and p was refined with constraints being imposed upon the isotropic displacement factors used for these sites and with restraints on the N—O bond lengths and O—N—O angles of each orientation. The water site O(4) also appears to have only partial occupancy, and this was set at 0.4 to give a reasonable value for its isotropic displacement factor. Hydrogen atoms for the cation were placed at calculated positions ($r = 0.95$ Å); these parameters were not refined in the crystallographic least-squares procedure but were recalculated periodically.

Least-squares refinement was performed using full-matrix methods minimizing the function $\sum w(|F_o| - |F_c|)^2$ where $w = [\sigma^2(F) + (0.0004)F^2]^{-1}$. Maximum and minimum heights in a final difference map were 0.51(2) and −0.31(2) e Å^{-3}, respectively, with the major features being close to nitrate 5. Data reduction and refinement computations were performed with XTAL3.2;[28] atomic scattering factors for neutral atoms and real and imaginary dispersion terms were taken from ref 29. Non-hydrogen positional parameters are given in Table

---

(27) A device similar to that described by: Inoue, Y.; Perrin, D. D. *J. Phys. Chem.* **1962**, *66*, 1689−1693.

(28) Hall, S. R.; Stewart, J. M., Eds. XTAL 2.4 User's Manual. Universities of Western Australia and Maryland, 1988.

Table 1. Crystal Data

chem formula	$C_{20}H_{54}CoN_{13}O_{18}$
fw	823.66
cryst syst	monoclinic
space group	$P2_1/n$
a, Å	14.382(4)
b, Å	14.604(6)
c, Å	16.998(6)
β, deg	100.28(3)
V, Å^3	3513(2)
Z	4
d_{calcd}, g cm^{-3}	1.557
μ(Mo Kα), cm^{-1}	5.8
T, °C	20(1)
cryst dimens, mm	0.11 × 0.31 × 0.09
X-radiation	Mo Kα
λ, Å	0.71073
data range, deg in 2θ	4−50
no. of unique data	6183
no. of data used in refinement	3168 [$I > 3\sigma(I)$]
no. of variables	459
no. of restraints	12
R^a	0.056
$R_w{}^b$	0.071
S^c	1.80
$F(000)$	1743.56

[a] $R = \sum||F_o| - |F_c||/\sum|F_o|$. [b] $R_w = [\sum w(|F_o| - |F_c|)^2/\sum(wF_o{}^2)]^{1/2}$. [c] $S = [\sum w(|F_o| - |F_c|)^2/(\text{no. of reflections} - \text{no. of variables})]^{1/2}$.

2 while interatomic distances and angles are given in Table 3. An ORTEP[30] drawing of the complex cation is given in Figure 1 showing 50% probability ellipsoids.

An X-ray crystal structure analysis of $[Co\{(NMe_3)_2sar\}]Cl_5{\cdot}6H_2O$ was also undertaken. The relevant crystal data are as follows: triclinic, $P\bar{1}$, $a = 14.156(2)$ Å, $b = 15.831(3)$ Å, $c = 19.637(4)$ Å, $\alpha = 100.94(1)°$, $\beta = 107.68(1)°$, $\gamma = 93.61(1)°$, $Z = 4$. The precision of this structure ($R = 0.11$, $R_w = 0.17$) suffered as a result of severe decomposition of the crystal during data collection. Nevertheless, solution of the structure of the chloride salt was achieved, which defined the same conformation in both crystallographically independent cations as that found in the structure of the nitrate salt. However, the precision of the structure relative to that of the nitrate salt was much less satisfactory, and full details are not reported.

Results

Syntheses. The cage complexes containing dimethylamino substituents were obtained in high yields from their amino precursors using standard methylation procedures involving either $HCHO/NaNCBH_3$/acetic acid in acetonitrile, or refluxing with HCOOH/HCHO. If excess quantities of the reagents were not used in the $HCHO/NaNCBH_3$ method, incompletely-methylated species were also obtained, but these have only been characterized by NMR spectroscopy. Pure chiral forms of the complexes were also prepared from their chiral precursors of known absolute configuration. The compounds were crystallized from 6 M HCl as their dimethylammonium complexes and microanalyses were in accord with the formulations. Quantitative methylation of the dimethylamino substituents was achieved by standard methods involving the reaction of the complexes with MeI in DMSO, or with dimethyl sulfate in DMF.

Table 2. Atomic Coordinates for $[Co\{(NMe_3)_2sar\}](NO_3)_5{\cdot}3H_2O$

	x/a	*y/b*	*z/c*
Co	0.08286(6)	0.23104(6)	0.21220(6)
N(1)	0.0520(4)	0.2204(4)	0.4732(3)
C(2)	0.0607(5)	0.2243(5)	0.3835(4)
C(3)	0.1036(5)	0.2355(5)	0.0409(4)
N(4)	0.1117(4)	0.2383(4)	−0.0496(3)
C(10)	0.0963(6)	0.3023(6)	0.5179(5)
C(11)	0.1657(5)	0.2036(5)	0.3774(4)
N(12)	0.1872(4)	0.2459(3)	0.3029(3)
C(13)	0.2763(5)	0.2096(5)	0.2804(4)
C(14)	0.2534(5)	0.1287(5)	0.2272(4)
N(15)	0.1662(4)	0.1493(4)	0.1655(3)
C(16)	0.1898(5)	0.1838(5)	0.0879(4)
C(17)	0.0920(5)	0.1460(6)	−0.0883(5)
C(20)	0.0998(6)	0.1357(6)	0.5137(5)
C(21)	−0.0053(4)	0.1514(5)	0.3362(4)
N(22)	0.0317(4)	0.1261(4)	0.2629(3)
C(23)	−0.0397(5)	0.0779(5)	0.2022(4)
C(24)	−0.0924(5)	0.1478(5)	0.1456(4)
N(25)	−0.0220(4)	0.2137(4)	0.1225(3)
C(26)	0.0115(4)	0.1841(5)	0.0489(4)
C(27)	0.0430(6)	0.3059(6)	−0.0950(5)
C(30)	−0.0506(5)	0.2185(6)	0.4822(5)
C(31)	0.0325(5)	0.3209(5)	0.3500(4)
N(32)	0.0049(4)	0.3162(4)	0.2611(3)
C(33)	0.0055(5)	0.4079(5)	0.2202(5)
C(34)	0.0994(5)	0.4234(5)	0.1961(4)
N(35)	0.1293(4)	0.3371(4)	0.1597(3)
C(36)	0.1007(5)	0.3352(5)	0.0707(4)
C(37)	0.2101(6)	0.2684(6)	−0.0590(5)
N(10)	0.3219(5)	0.4231(5)	0.4031(4)
O(11)	0.3902(4)	0.4771(4)	0.4207(4)
O(12)	0.2449(4)	0.4489(4)	0.3653(4)
O(13)	0.3288(5)	0.3431(4)	0.4230(5)
N(20)	0.3546(5)	0.0692(5)	0.5019(5)
O(21)	0.3623(4)	0.1528(4)	0.5104(4)
O(22)	0.3001(6)	0.0363(5)	0.4463(6)
O(23)	0.4009(7)	0.0177(5)	0.5485(5)
N(30)	0.3678(5)	0.4195(5)	0.1539(5)
O(31)	0.3268(4)	0.3505(4)	0.1227(4)
O(32)	0.3450(5)	0.4522(5)	0.2140(4)
O(33)	0.4313(6)	0.4547(5)	0.1243(5)
N(40)	0.2557(6)	0.1761(7)	0.7307(5)
O(41)	0.3061(5)	0.2138(7)	0.7858(5)
O(42)	0.2891(5)	0.1589(7)	0.6711(5)
O(43)	0.1724(5)	0.1571(9)	0.7310(5)
N(50A)[a]	0.6668(9)	−0.027(1)	0.073(1)
O(51A)[a]	0.600(1)	−0.012(1)	0.1059(9)
O(52A)[a]	0.660(1)	−0.081(1)	0.0165(8)
O(53A)[a]	0.7387(9)	0.017(1)	0.095(1)
N(50B)[b]	0.673(1)	−0.009(2)	0.083(1)
O(51B)[b]	0.591(1)	−0.034(2)	0.062(2)
O(52B)[b]	0.726(2)	−0.011(2)	0.034(2)
O(53B)[b]	0.696(2)	0.036(2)	0.145(1)
O(1)	0.8044(7)	0.0357(6)	0.3695(7)
O(2)	0.4405(8)	0.086(1)	0.1328(9)
O(3)[a]	0.660(1)	0.108(1)	0.238(1)
O(4)[b]	0.501(2)	0.226(2)	0.210(1)

[a] Occupancy 0.650(8). [b] Occupancy 0.350(8). [c] Occupancy 0.4.

X-ray Crystallographic Analysis of $[Co\{(NMe_3)_2sar\}](NO_3)_5{\cdot}3H_2O$. The drawing of the complex cation (Figure 1) clearly shows that the pendent primary amines have undergone permethylation. A striking feature of the structure is that the complex adopts an *ob*$_3$ arrangement of its five-membered chelate rings.[31] The average Co−N bond length (1.961(6) Å) does not differ greatly from those identified in other sar-type cobalt(III) complexes or from that found in the structural analysis of the chloride salt. However, all N−Co−N angles in the present structure are within ~3° of their ideal values for octahedral symmetry of the CoN_6 core, and the trigonal twist angle of the

---

(29) *International Tables for X-ray Crystallography*; Kynoch Press: Birmingham, England, 1974; Vol. 4, pp 61−66, 99−101, 149−150.

(30) Johnson, C. K. *ORTEP II*; Report ORNL-5138; Oak Ridge National Laboratory: Oak Ridge, TN, 1971. Davenport, G.; Hall, S. R.; Dreissig, W. *ORTEP*, in ref 28.

(31) Strictly speaking, one should refer to the overall symmetry of the *lel*$_3$ and *ob*$_3$ conformations, i.e. D_3 or C_3 which arises from the helicity of the two caps. In addition, it is known that there are two quite different D_3*lel*$_3$ conformations: one is close to octahedral while the other exhibits a large trigonal twist distortion. This distinction will be made when necessary.

Table 3. Interatomic Distances (Å) and Angles (deg) for $[Co\{(NMe_3)_2sar\}](NO_3)_5 \cdot 3H_2O$[a]

Co—N(12)	1.962(5)	Co—N(22)	1.965(6)	Co—N(32)	1.956(6)
Co—N(15)	1.957(6)	Co—N(25)	1.960(5)	Co—N(35)	1.963(6)
N(1)—C(2)	1.553(9)	C(3)—N(4)	1.563(9)		
N(1)—C(10)	1.50(1)	N(1)—C(20)	1.52(1)	N(1)—C(30)	1.51(1)
C(2)—C(11)	1.56(1)	C(2)—C(21)	1.55(1)	C(2)—C(31)	1.55(1)
C(3)—C(16)	1.546(9)	C(3)—C(26)	1.55(1)	C(3)—C(36)	1.55(1)
N(4)—C(17)	1.50(1)	N(4)—C(27)	1.51(1)	N(4)—C(37)	1.52(1)
C(11)—N(12)	1.489(9)	C(21)—N(22)	1.49(1)	C(31)—N(32)	1.494(9)
N(12)—C(13)	1.497(9)	N(22)—C(23)	1.495(8)	N(32)—C(33)	1.510(9)
C(13)—C(14)	1.49(1)	C(23)—C(24)	1.51(1)	C(33)—C(34)	1.50(1)
C(14)—N(15)	1.515(8)	C(24)—N(25)	1.500(9)	C(34)—N(35)	1.500(9)
N(15)—C(16)	1.51(1)	N(25)—C(26)	1.48(1)	N(35)—C(36)	1.494(9)
N(10)—O(11)	1.253(8)	N(10)—O(12)	1.236(8)	N(10)—O(13)	1.216(9)
N(20)—O(21)	1.23(1)	N(20)—O(22)	1.21(1)	N(20)—O(23)	1.20(1)
N(30)—O(31)	1.238(9)	N(30)—O(32)	1.22(1)	N(30)—O(33)	1.23(1)
N(40)—O(41)	1.21(1)	N(40)—O(42)	1.22(1)	N(40)—O(43)	1.23(1)
N(50A)—O(51A)	1.22(2)	N(50A)—O(52A)	1.23(2)	N(50A)—O(53A)	1.22(2)
N(50B)—O(51B)	1.23(3)	N(50B)—O(52B)	1.22(4)	N(50B)—O(53B)	1.23(4)

N(12)—Co—N(15)	87.0(2)	N(22)—Co—N(25)	86.8(2)	N(32)—Co—N(35)	87.7(2)
N(12)—Co—N(22)	92.0(2)	N(22)—Co—N(32)	91.2(2)	N(12)—Co—N(32)	90.7(2)
N(12)—Co—N(25)	178.8(2)	N(22)—Co—N(35)	177.9(2)	N(15)—Co—N(32)	177.2(2)
N(12)—Co—N(35)	89.8(2)	N(15)—Co—N(22)	90.4(2)	N(25)—Co—N(32)	89.6(2)
N(15)—Co—N(25)	92.7(2)	N(25)—Co—N(35)	91.4(2)	N(15)—Co—N(35)	90.8(2)
C(2)—N(1)—C(10)	111.5(6)	C(2)—N(1)—C(20)	111.5(6)	C(2)—N(1)—C(30)	110.6(5)
C(10)—N(1)—C(20)	107.6(5)	C(10)—N(1)—C(30)	107.4(6)	C(20)—N(1)—C(30)	108.1(6)
N(1)—C(2)—C(11)	107.8(5)	N(1)—C(2)—C(21)	109.5(6)	N(1)—C(2)—C(31)	109.5(6)
C(11)—C(2)—C(21)	110.0(6)	C(11)—C(2)—C(31)	110.2(6)	C(21)—C(2)—C(31)	109.8(5)
N(4)—C(3)—C(16)	109.1(6)	N(4)—C(3)—C(26)	108.3(5)	N(4)—C(3)—C(36)	108.0(6)
C(16)—C(3)—C(26)	109.7(6)	C(16)—C(3)—C(36)	110.9(5)	C(26)—C(3)—C(36)	110.7(6)
C(3)—N(4)—C(17)	111.4(6)	C(3)—N(4)—C(27)	111.3(6)	C(3)—N(4)—C(37)	110.2(5)
C(17)—N(4)—C(27)	107.9(5)	C(17)—N(4)—C(37)	108.6(6)	C(27)—N(4)—C(37)	107.1(6)
C(2)—C(11)—N(12)	109.0(5)	C(2)—C(21)—N(22)	109.1(5)	C(2)—C(31)—N(32)	109.5(6)
Co—N(12)—C(11)	112.2(4)	Co—N(22)—C(21)	113.1(4)	Co—N(32)—C(31)	113.0(4)
Co—N(12)—C(13)	109.3(4)	Co—N(22)—C(23)	109.2(4)	Co—N(32)—C(33)	108.5(5)
C(11)—N(12)—C(13)	112.8(5)	C(21)—N(22)—C(23)	113.1(5)	C(31)—N(32)—C(33)	113.7(5)
N(12)—C(13)—C(14)	109.2(5)	N(22)—C(23)—C(24)	109.0(6)	N(32)—C(33)—C(34)	109.8(6)
C(13)—C(14)—N(15)	109.2(6)	C(23)—C(24)—N(25)	108.3(5)	C(33)—C(34)—N(35)	109.0(6)
Co—N(15)—C(14)	109.4(4)	Co—N(25)—C(24)	109.9(4)	Co—N(35)—C(34)	109.2(4)
Co—N(15)—C(16)	113.7(4)	Co—N(25)—C(26)	112.0(4)	Co—N(35)—C(36)	113.0(4)
C(14)—N(15)—C(16)	112.6(5)	C(24)—N(25)—C(26)	111.7(5)	C(34)—N(35)—C(36)	112.7(5)
C(3)—C(16)—N(15)	109.3(6)	C(3)—C(26)—N(25)	110.1(5)	C(3)—C(36)—N(35)	109.3(5)
O(11)—N(10)—O(12)	121.6(6)	O(11)—N(10)—O(13)	121.1(6)	O(12)—N(10)—O(13)	117.3(7)
O(21)—N(20)—O(22)	121.1(7)	O(21)—N(20)—O(23)	120.9(7)	O(22)—N(20)—O(23)	118.0(8)
O(31)—N(30)—O(32)	119.9(8)	O(31)—N(30)—O(33)	119.7(8)	O(32)—N(30)—O(33)	120.5(8)
O(41)—N(40)—O(42)	117.8(9)	O(41)—N(40)—O(43)	123(1)	O(42)—N(40)—O(43)	118.9(9)
O(51A)—N(50A)—O(52A)	121(2)	O(51A)—N(50A)—O(53A)	118(2)	O(52A)—N(50A)—O(53A)	121(2)
O(51B)—N(50B)—O(52B)	119(3)	O(51B)—N(50B)—O(53B)	120(3)	O(52B)—N(50B)—O(53B)	119(3)

[a] Restraints imposed on orientations A and B of nitrate 5 during refinement: distance N—O = 1.22(1) Å; angle O—N—O = 120(1)°.

two planes of three N atoms perpendicular to the C_3 axis is 57.8(3)°, i.e. ~2° from an ideal octahedral array. There is also a slight compression of the CoN_6^{3+} core along the trigonal axis defined by the average polar angle subtended by the Co—N bond and the C_3 axis; $\alpha = 55.8(3)°$ compared with 54.7° for an ideal octahedron. These results are to be compared to those of structures of the *lel*$_3$-conformations of $[Co\{(NH_3)_2sar\}]^{5+}$ in two lattices,[32] $[Co\{(NO_2)_2sar\}]^{3+}$,[33] $[Co\{(ZnCl_3)sar\}]^{+}$,[34] and $[Co\{(HO)_2sar\}]^{3+}$ [33] in different lattices, and the *ob*$_3$-conformations of $[Co\{(NH_2OH)_2sar\}]^{5+}$,[35] $[Co\{(NO_2)_2sar\text{-}H\}]^{2+}$ [3] and the somewhat less relevant $[Co(Me\text{-}arsasar)]^{3+}$ ion[36] in separate lattices. Detailed comparisons of these structures are made in the Discussion section.

Spectra. ^1H NMR spectra of the complexes exhibited sharp singlets at 2.98 ppm ($N(\mathbf{CH}_3)_2$), 3.03 ppm ($HN(\mathbf{CH}_3)_2^+$) and 3.30 ppm ($N(\mathbf{CH}_3)_3^+$), typical of dimethylamino, dimethylammonium, and trimethylammonium substituents, respectively. The integrations were in accord with the above formulations. The N—H signals of the coordinated amine groups remained in 36% DCl/D_2O at ~7.0 ppm, showing that methylation occurs at the uncoordinated amino substituents and not the coordinated secondary amine groups. For the symmetric cage complexes in D_2O the ^1H NMR spectra consist of an AB doublet of doublets for the CH_2 groups of the caps and an AA'BB' coupling pattern for the CH_2 groups of the 1,2-ethanediamine components of the cage. More complex coupling patterns were observed for the unsymmetrically-substituted cage complexes. No ^1H NMR signals were observed for the NH protons of the $-NH_3^+$ or $NHMe_2^+$ substituents in either 36% DCl/D_2O or in D_2O. Therefore, the protons of these groups are more acidic and have exchanged within the time required to collect the spectrum (time scale of minutes). The ^1H-decoupled ^{13}C NMR spectra of the symmetric cage complexes show an extra singlet due to the dimethylamino and trimethylamino substituents, in addition to the other three resonances typical of the cage backbone.[3,5,25,26]

---

(32) Geue, R. J.; Sargeson, A. M.; Snow, M. R.; White, A. H. To be submitted for publication.

(33) Clark, I. J.; Geue, R. J.; Engelhardt, L. M.; Harrowfield, J. M.; Sargeson, A. M.; White, A. H. *Aust. J. Chem.* **1993**, *46*, 1485–1505.

(34) Creaser, I. I.; Lydon, J. D.; Sargeson, A. M.; Horn, E.; Snow, M. R. *J. Am. Chem. Soc.* **1984**, *106*, 5729–5731.

(35) Balahura, R. J.; Ferguson, G.; Ruhl, B. L.; Wilkins, R. J. *Inorg. Chem.* **1983**, *22*, 3990–3992.

(36) Höhn, A.; Geue, R. J.; Sargeson, A. M.; Willis, A. C. *J. Chem. Soc., Chem. Commun.* **1989**, 1648–1649.

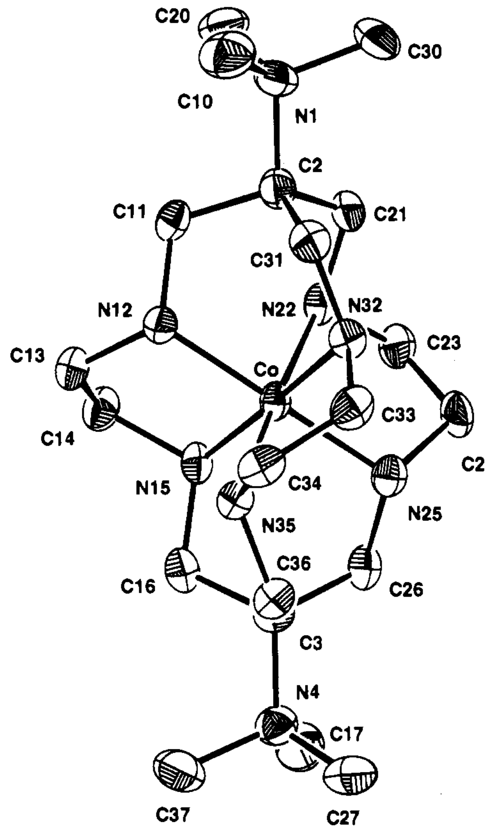

Figure 1. Drawing of the [Co{$(NMe_3)_2$sar}]$^{5+}$ ion (H atoms have been omitted for clarity).

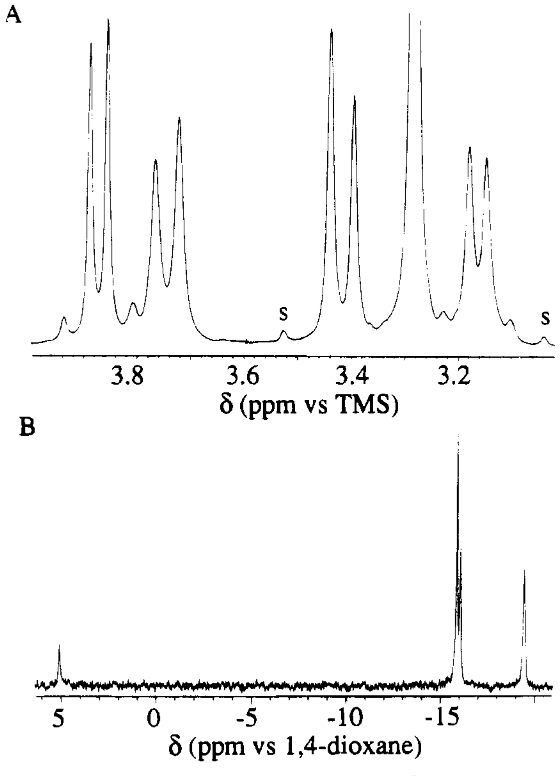

Figure 2. NMR spectra of [Co{$(NMe_3)_2$sar}]$^{5+}$ in D_2O: (A) ^{1}H spectrum; (B) ^{1}H-decoupled ^{13}C spectrum.

The two different CH_2 resonances were assigned from the ^{1}H—^{13}C 2D NMR spectra. Figure 2 shows the ^{1}H and ^{1}H-decoupled ^{13}C NMR spectra of [Co{$(NMe_3)_2$sar}]$^{5+}$ which illustrate these features. A comparison of the spectra of [Co{$(NMe_3)_2$sar}]$^{5+}$ with those of "fixed conformation" analogues[22] is given in Table 4.

There is little difference in the ^{13}C chemical shifts of the CH_3 groups of the dimethylammonium groups on protonation, but progressive methylation of the amine substituents moves the CH_3 resonances downfield by ~11.5 ppm per methylation, i.e. as follows: $-NH_2Me^+$, $\delta = -38.8$ ppm; $-NHMe_2^+$, $\delta = -27.2$ ppm; NMe_3^+, $\delta = -15.7$ ppm. Therefore, the position of this resonance is diagnostic for each of these different groups and will be useful for characterizing isomers of partially-methylated cage complexes. Similarly, the position of the quaternary carbon signal is diagnostic of the degree of methylation, i.e., as follows: CNH_2Me^+, $\delta = -6.9$ ppm; $CNHMe_2^+$, $\delta = -1.1$ ppm; $CNMe_3^+$, $\delta = +5.1$ ppm. Apart from these features, there was an upfield shift in the resonance of the CH_2 (en) groups on di- or trimethylation of the ammonium substituents. This is significant since the chemical shift of this resonance is virtually invariant over a large range of substituents apart from those in question.[3,25,26] A similar shift was seen in the presumably conformationally stable Me_3sar cage complexes in going from the *lel*$_3$ to the *ob*$_3$ conformation.[22] With cage complexes containing only one dimethylammonium, or one methylammonium and one dimethylammonium substituent, the upfield shifts in the value of this ^{13}C NMR resonance were between these two extremes. The CH_2 resonances of the cap show a similar trend with the degree of methylation of the amine substituent, however the differences in chemical shifts are smaller than those described above.

Methylation of the pendent primary amines of [Co{$(NH_3)_2$sar}]$^{5+}$ had a marked effect on the solution electronic spectrum, where a progressive hypsochromic shift of the two d−d electronic transitions was observed upon methylation of [Co{$(NH_3)_2$sar}]$^{5+}$ to form [Co{$(NHMe_2)_2$sar}]$^{5+}$ and then [Co{$(NMe_3)_2$sar}]$^{5+}$ (Table 5). In addition to the change in color, the intensity of the lower energy d−d maximum of [Co{$(NMe_3)_2$sar}]$^{5+}$ is reduced to *ca.* 60% of the intensity of the corresponding transition in [Co{$(NH_3)_2$sar}]$^{5+}$. Deprotonation of the pendent amines of [Co{$(NH_3)_2$sar}]$^{5+}$ or [Co{$(NHMe_2)_2$sar}]$^{5+}$ has little effect on the energies of the electronic absorption maxima, although it does result in the higher energy d−d maximum of the latter complex being obscured by charge transfer transitions in the UV region.

By contrast, deprotonation of one coordinated amine in [Co{$(NMe_3)_2$sar}]$^{5+}$ was observed when the spectrum was measured in 0.1 M NaOH solution which resulted in a bathochromic shift of the d−d electronic maxima to 510 and 363 nm. A pK_a value of 8.65 (I = 0.1 M NaCl at 25 °C) was determined for this process by potentiometric titration. A similarly low pK_a for a coordinated secondary amine was identified in [Co{$(NO_2)_2$sar}]$^{3+}$ where the deprotonated form was characterized by an X-ray crystal structure.[3] The presence of the strongly electron-withdrawing $-NMe_3^+$ and $-NO_2$ groups is a critical factor in enhancing the acidity of the coordinated secondary amines. By comparison, no deprotonation of the secondary amines of [Co{$(NH_2)_2$sar}]$^{3+}$ or [Co{$(NMe_2)_2$sar}]$^{3+}$ was identified below pH 12.

Methylation of the pendent primary amine substituents of optically active [Co{$(NH_3)_2$sar}]$^{5+}$, to form [Co{$(NHMe_2)_2$sar}]$^{5+}$ and then [Co{$(NMe_3)_2$sar}]$^{5+}$, resulted in essentially inversion of the visible CD maxima of both derivatives relative to the parent complex of the same absolute configuration (Figure 3). The effects on the CD spectra through methylation and protonation of these amine substituents, and by substitutions on the ligand backbone are also shown in Table 6.

Redox Chemistry. The reversible reduction potentials (ΔE_p ~ 60−70 mV at 50 mV s^{-1}, derived from cyclic voltammetry) exhibited by the various amine-substituted cage complexes are

Table 4. Characteristic ^{13}C NMR Resonances of Cobalt Cage Complexes[a]

complex	C_{apical}	CH_2 (en)	CH_2 (cap)	CH_3 (amine)	CH_3 (cap)
$[Co\{(NH_2)_2sar\}]^{3+}$	−10.3	−11.6	−11.6		
$[Co\{(NH_2,Me)sar\}]^{3+}$	−10.2 (NH_2), −24.5 (CH_3)	−11.6	−11.6		−47.0
$[Co\{(NH_3)_2sar\}]^{5+}$	−10.3	−11.7	−15.6		
$[Co\{(NH_3,Me)sar\}]^{4+}$	−10.4 (NH_3^+), −24.0 (CH_3)	−11.7	−11.7 (CH_3), 15.5 (NH_3^+)		−47.3
$[Co\{(NMe_2)_2sar\}]^{3+}$	−3.3	−15.5	−16.5	−28.1	
$[Co\{(NMe_2,Me)sar\}]^{3+}$	−3.1 (NMe_2), −24.4 (CH_3)	−12.6	−11.7 (CH_3), −16.6 (NMe_2)	−28.0	−45.9
$[Co\{(NHMe_2,NH_2Me)sar\}]^{5+}$	−1.0 ($NHMe_2^+$), −6.9 (NH_2Me^+)	−14.7	−17.3 (NH_2Me^+), −18.3 ($NHMe_2^+$)	−27.3, −38.8[b]	
$[Co\{(NHMe_2)_2sar\}]^{5+}$	−1.7	−15.7	−18.6	−27.1	
$[Co\{(NHMe_2,Me)sar\}]^{4+}$	−1.2 ($NHMe_2^+$), −24.7 (CH_3)	−13.1	−12.2 (CH_3), −18.1 ($NHMe_2^+$)	−27.0	47.0
$[Co\{(NMe_3)_2sar\}]^{5+}$	+5.2	−16.0	−19.5	−15.9	
$[Co\{(NMe_3,Me)sar\}]^{4+}$	+5.3 (NMe_3^+), −24.3 (CH_3)	−15.6	−12.3 (CH_3), −19.1 (NMe_3^+)	−15.6	−47.1
fac-lel$_3$-$[Co\{(NH_2)_2Me_3sar\}]^{3+}$	−9.4, −10.4	−3.4, −5.5	−12.6, −13.3		
fac-lel$_3$-$[Co\{(NH_3)_2Me_3sar\}]^{5+}$	−9.1, −10.2	−3.3, −5.4	−16.4, −17.3		
fac-ob$_3$-$[Co\{(NH_2)_2Me_3sar\}]^{3+}$	−9.9, −11.7	−9.7, −11.5	−11.6, −18.3		
fac-ob$_3$-$[Co\{(NH_3)_2Me_3sar\}]^{5+}$	−9.6, −11.4	−9.6, −11.4	−16.2, −22.1		

[a] Downfield shifts *vs* 1,4-dioxane as an internal standard (ppm). [b] The resonance at −27.3 ppm is assigned to the $NHMe_2^+$ group.

Table 5. UV/Vis Absorption Spectra of the Cage Complexes[a]

complex	charge transfer	d−d bands
$[Co\{(NH_2)_2sar\}]^{3+}$ [b]	222, 240	343 (130), 475 (150)
$[Co\{(NH_3)_2sar\}]^{5+}$ [c]	232	344.5 (150), 475 (150)
$[Co\{(NMe_2)_2sar\}]^{3+}$ [b]		456 (113)
$[Co\{(NHMe_2)_2sar\}]^{5+}$ [c]	233 (19 500)	454 (104)
$[Co\{(NMe_3)_2sar\}]^{5+}$ [c]	231 (10 800)	329 (110), 445 (94.4)
$[Co\{(NH_3,Me)sar\}]^{4+}$ [c]		345 (123), 472 (139)
$[Co\{(NMe_2,Me)sar\}]^{3+}$ [b]		473 (164)
$[Co\{(NHMe_2,Me)sar\}]^{4+}$ [c]	240 (18 300)	340 (134), 470 (151)
fac-lel$_3$-$[Co\{(NH_2)_2Me_3sar\}]^{3+}$ [b]		340 sh (178), 474 (148)
fac-ob$_3$-$[Co\{(NH_2)_2Me_3sar\}]^{3+}$ [b]		330 sh (107), 450 (83)
fac-lel$_3$-$[Co\{(NH_3)_2Me_3sar\}]^{5+}$ [d]	246 (19 500)	346 (135), 480 (152)
fac-ob$_3$-$[Co\{(NH_3)_2Me_3sar\}]^{5+}$ [d]	231 (19 300)	331 (93.8), 450 (81.4)

[a] λ_{max}, nm; molar absorption coefficients in parentheses ($M^{-1}\ cm^{-1}$). [b] pH 7. [c] 0.1 M HCl. [d] 0.1 M CF_3SO_3H.

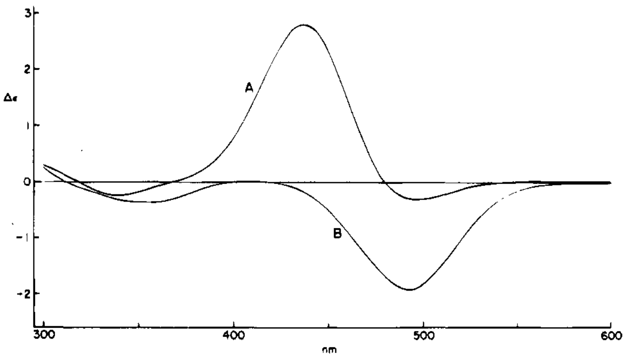

Figure 3. Circular dichroism spectra of the Λ Isomers of (A) $[Co\{(NMe_3)_2sar\}]^{5+}$ (H_2O) and (B) $[Co\{(NH_3)_2sar\}]^{5+}$ (0.1 HCl).

Table 6. Circular Dichroism Data for Relevant Co(III) Complexes

	CD maxima		
Λ complex	Δε, $M^{-1}\ cm^{-1}$	λ, nm	charge
$(+)_D$-$[Co(en)_3]Cl_3{\cdot}NaCl{\cdot}6H_2O$[a]	+1.94	489	3+
	−0.14	429	
	+0.226	350	
$(-)_D$-$[Co\{(NH_3)_2sar\}]Cl_5{\cdot}H_2O$[b]	−2.520	473	3+
	−0.162	364	
$(-)_D$-$[Co\{(NH_3)_2sar\}]Cl_5{\cdot}H_2O$[c]	−1.891	491	5+
	−0.347	351	
$(+)_D$-$[Co\{(NHMe_2)_2sar\}]Cl_5{\cdot}4H_2O$[b]	−0.402	498	3+
	+1.779	439	
$(+)_D$-$[Co\{(NHMe_2)_2sar\}]Cl_5{\cdot}4H_2O$[c]	−0.588	497	5+
	+1.851	440	
	−0.331	338	
$(+)_D$-$[Co\{(NMe_3)_2sar\}]Cl_5{\cdot}6H_2O$[a]	−0.298	495	5+
	+2.724	436	
	−0.238	337	
fac-(*S*)$_3$-*lel*$_3$-$[Co\{(NH_3)_2Me_3sar\}](CF_3SO_3)_5$[d]	−2.92	491	5+
	−0.052	399	
	−0.31	360	
fac-(*R*)$_3$-*ob*$_3$-$[Co\{(NH_3)_2Me_3sar\}](CF_3SO_3)_5$[d]	+3.52	451	5+
	−0.19	340	

[a] H_2O. [b] Aqueous Hepes buffer, pH 7.3, $I = 0.2$ M. [c] 0.1 M HCl. [d] 0.1 M CF_3SO_3H.

Table 7. Redox Potentials for the Co(III/II) Couples of the Cage Complexes with Amine and Ammonium Substituents

	$E_{1/2}$, V vs NHE		
redox couple	pH 1.0[a]	0.1 M $NaClO_4$	pH 7.5[b]
$[Co(sep)]^{3+/2+}$		−0.256	
fac-ob$_3$-$[Co\{(NH_2)_2Me_3sar\}]^{3+/2+}$	−0.32		−0.64
fac-lel$_3$-$[Co\{(NH_2)_2Me_3sar\}]^{3+/2+}$	+0.02		−0.32
$[Co\{(NH_2)_2sar\}]^{3+/2+}$	+0.02		−0.35
	+0.059[c]		−0.299[d]
lel$_3$-$[Co\{(NH_2)_2char\}]^{3+/2+}$ [e]	0.00		−0.35
$[Co\{(NHMe_2,NH_2Me)sar\}]^{5+/4+}$	+0.054[c]		
$[Co\{(NMe_2)_2sar\}]^{3+/2+}$	+0.055[c]		−0.293[d]
$[Co\{(NMe_3)_2sar\}^{5+/4+}$		+0.051	
$[Co\{(NH_2,Me)sar\}]^{3+/2+}$	−0.186[c]		−0.347[d]
$[Co\{(NMe_2,Me)sar\}]^{3+/2+}$	−0.189[c]		−0.341[d]

[a] All primary amines protonated. [b] No primary amines protonated. [c] 0.05 M $HClO_4$/0.05 M $NaClO_4$. [d] 0.10 M $NaClO_4$, pH adjusted to 7 after dissolution of the complex. [e] Cage complex derived from *lel*$_3$-$[Co(\textit{trans}\text{-}1,2\text{-cyclohexanediamine})_3]^{3+}$.

given in Table 7. The reduction potentials of the methylated cage complexes are shifted by *ca.* +150 mV per substituent upon protonation or permethylation of the neutral amine. The electron self-exchange rate constants for the $[Co\{(NMe_3)_2sar\}]^{5+/4+}$ couple at 25 °C are 0.011(1) $M^{-1}\ s^{-1}$ (I = 0.2 M NaCl) and 0.014(1) $M^{-1}\ s^{-1}$ (I = 1.0 M NaCl). These are the smallest rate constants that have been measured for cobalt complexes of sar-type ligands to date under the same conditions (Table 8). They are about 2-fold smaller than that for the $[Co\{(NH_3)_2sar\}]^{5+/4+}$ couple (0.025 $M^{-1}\ s^{-1}$), which has the same set of charges and the same $Co^{III/II}$ redox potential as the permethylated complex.

Discussion

Conformational Structures of the Co(III) Complexes from Spectroscopic Measurements. The relative changes in the chemical shifts of the ^{13}C NMR resonances of the "en" carbons of $[Co\{(NMe_3)_2sar\}]^{5+}$ and $[Co\{(NH_3)_2sar\}]^{5+}$ are similar to those of the conformationally stabilized *ob*$_3$ and *lel*$_3$-*fac*-$[Co\{(NH_3)_2Me_3sar\}]^{5+}$ complexes, respectively.[22] (Table 4). Similarly, the electronic spectral properties of $[Co\{(NMe_3)_2sar\}]^{5+}$ are very similar to those of *ob*$_3$-*fac*-$[Co\{(NH_3)_2Me_3$-

Table 8. Electron Self-Exchange Rate Constants at 25 °C and I = 0.2 M for Co(III/II) Couples of Cage Complexes

couple	k, M^{-1} s^{-1}	ref
$[Co(sep)]^{3+/2+}$	5.1	4
fac-ob$_3$-$[Co\{(NH_3)_2Me_3sar\}]^{5+/4+}$	0.97	22
lel$_3$-$[Co\{(NH_3)_2char\}]^{5+/4+}$	0.038	12
fac-lel$_3$-$[Co\{(NH_3)_2Me_3sar\}]^{5+/4+}$	0.031	22
$[Co\{(NH_3)_2sar\}]^{5+/4+}$	0.025	10
$[Co\{(NMe_3)_2sar\}]^{5+/4+}$	0.011	This work

sar}]$^{5+}$ and quite different from those with a *lel*$_3$ or *lel*$_2$*ob*[24] conformation (Table 5). Apart from the difference in the frequency of this absorption, the weaker intensity of the absorption band of $^1T_{1g} \leftarrow {}^1A_{1g}$ (O_h) origin of the putative *ob*$_3$ conformer as compared to the *lel*$_3$ conformer is consistent with the former having a CoN_6^{3+} chromophore whose symmetry is closer to octahedral. Therefore, stronger symmetry selection rules for the transition apply. However, the most convincing evidence for the solution structure of $[Co\{(NMe_3)_2sar\}]^{5+}$ lies in the CD spectral properties which are similar to those of *ob*$_3$-*fac*-$[Co\{(NH_3)_2Me_3sar\}]^{5+}$ and inverted with respect to $[Co\{(NH_3)_2sar\}]^{5+}$ and *lel*$_3$-*fac*-$[Co\{(NH_3)_2Me_3sar\}]^{5+}$ for the same absolute configuration about Co. From all of this data, it is inferred that $[Co\{(NMe_3)_2sar\}]^{5+}$ exists mainly as the *ob*$_3$ isomer in aqueous media and that $[Co\{(NH_3)_2sar\}]^{5+}$ is in the *lel*$_3$ or *lel*$_2$*ob* conformation. The salient features of the solution CD spectra reflect the sum of the $^1E_1 \leftarrow {}^1A_1$ and $^1A_2 \leftarrow {}^1A_1$ components derived from the $^1T_{1g} \leftarrow {}^1A_{1g}$ (O_h) transition in the reduced D_3 symmetry ligand field, where both components are CD active and are of opposite sign. In the Λ configuration, the sign of the $^1E_1 \leftarrow {}^1A_1$ component is positive and that of the $^1A_2 \leftarrow {}^1A_1$ component is negative for both the $[Co(en)_3]^{3+}$ and $[Co(sep)]^{3+}$ ions.[37] It is presumed that the same relationship holds for the complexes discussed here, but it is known that the difference between the rotational strengths of the two components is sensitive to a number of factors. For example, the absolute magnitude of the $^1E_1 \leftarrow {}^1A_1$ component is larger than that of the $^1A_2 \leftarrow {}^1A_1$ component in the spectrum of Λ-$[Co(en)_3]^{3+}$, but the opposite is the case[37] for Λ-$[Co(sep)]^{3+}$. In solution, this gives rise to a net positive CD band at 489 nm for Λ-$[Co(en)_3]^{3+}$ and a net negative CD band at ~460 nm for Λ-$[Co(sep)]^{3+}$. In the present instance, Λ-$[Co\{(NH_3)_2sar\}]^{5+}$ shows a net negative CD band at ~490 nm, whereas Λ-$[Co\{(NMe_3)_2sar\}]^{5+}$ shows a net positive CD band at ~440 nm. Therefore, the net CD signal that is observed is the difference between two large CD signals from the $^1A_2 \leftarrow {}^1A_1$ and $^1E \leftarrow {}^1A_1$ transitions of approximately equal area but of opposite sign. This makes assignment of the absolute configuration on the basis of the sign of the solution CD signal alone hazardous and these results point to the sensitivity of this technique towards small structural variations.

The CD of these ions arises from the stereogenic Co (Λ or Δ) and N-donor (*R* or *S*) centers, the chirality of the conformationally labile five-membered chelate rings (λ or δ), and the helicity of the trigonal caps (*R* or *S*). Interconversion between the *lel* and *ob* chelate rings does not alter any of the stereogenic centers. Therefore, the CD change is only a function of the *lel* to *ob* conformational change and consequent orientation of the caps. These changes are reflected in both the rotational strengths of the $^1A_2 \leftarrow {}^1A_1$ and $^1E \leftarrow {}^1A_1$ transitions (both in D_3 symmetry) and their energy separations in the spectrum. Presumably, this effect is manifested largely through small changes in the bond lengths and atom or orbital orientations, and consequently, in the manner in which these influence the electric and magnetic moments of the transitions of d−d origin.

The ^{13}C NMR chemical shifts of the CH_2 (en) carbon atoms of $[Co\{(NHMe_2)_2sar\}]^{5+}$ are similar to those of $[Co\{(NMe_3)_2sar\}]^{5+}$, which appears to be mainly *ob*$_3$ in solution. The electronic spectral properties of $[Co\{(NHMe_2)_2sar\}]^{5+}$ are intermediate between those found for the conformationally fixed *ob*$_3$ and *lel*$_3$-$[Co\{(NH_3)_2Me_3sar\}]^{5+}$ cage complexes. The CD spectrum of $[Co\{(NHMe_2)_2sar\}]^{5+}$ resembles those of the *ob*$_3$ cage complexes more than those of the *lel*$_3$ cage complexes of the same absolute configuration (Table 5). However, the lower energy d−d electronic maxima of conformationally stabilized *ob*$_3$- and *ob*$_2$*lel*-$[Co\{(NH_3)_2Me_3sar\}]^{5+}$ are found at 450 and 475 nm respectively.[22,24] On this basis, it is likely that the $[Co\{(NHMe_2)_2sar\}]^{5+}$ complex (λ_{max} 454 nm) exists in aqueous solution largely in the *ob* condition.

Conformer Stability and Spectral Properties. The solution electronic spectra of the *ob*$_3$ and *lel*$_3$ Co(III) cages have been shown to differ markedly, with the former exhibiting a stronger ligand field whereas the latter display electronic maxima more typical of hexaaminecobalt(III) complexes. However, it emerges from X-ray structural analyses that the Co−N bond lengths in *ob*$_3$-$[Co\{(NMe_3)_2sar\}]^{5+}$ are not very different from those found in *lel*$_3$-$[Co\{(X,Y)sar\}]^{m+}$ ($X = Y = NH_3$, $m = 5$; $X = Y = NO_2$, $m = 3$; $X = ZnCl_3$, $Y = H$, $m = 1$). Therefore, variations in the Co−N bond lengths on going from *ob*$_3$ to *lel*$_3$ are not a sensitive gauge for the observed spectral changes. However, the structure of $[Co\{(NMe_3)_2sar\}]^{5+}$ did reveal that the symmetry of the CoN_6 core is very close to octahedral, whereas the structures of analogous *lel*$_3$ conformers show greater distortions from octahedral symmetry, i.e. trigonal twist angles of ~54°.

Although the *ob*$_3$ conformation has been observed in the crystal structures of $[Co\{(NH_2OH)_2sar\}]Cl_5{\cdot}4H_2O$,[32] $[Co\{(NO_2)_2sar\text{-}H\}]Cl_2{\cdot}4H_2O$,[3] and $[Co(Me\text{-}arsasar)](PF_6)_3{\cdot}3H_2O$,[36] electronic spectroscopy indicates that the hydroxylamine complex is mainly in the *lel* conformation in solution,[38] the deprotonated dinitro complex cannot be evaluated because of the hypsochromic shift in the electronic maxima upon deprotonation, and the arsasar complex apparently retains its *ob* conformational character in solution. The last example is probably not particularly relevant since the long As−C bond lengths in the cap, compared with the C−C and N−C bonds found in sar- and sep-type cages, may influence the outcome in this case. However, the $[Co\{(NO_2)_2sar\}]^{3+}$ ion is *lel*$_3$ in the lattice[33] and in solution exhibits physical properties consistent with conformations which are dominantly of the *lel* form.

As for the solution behavior of the Co(II) complexes, not enough is known about the electronic spectroscopy of complexes of this type yet to obtain information on the preferred conformers in solution, and NMR spectroscopy of these strongly paramagnetic complexes is also unlikely to be useful in determining solution conformations. By analogy with the X-ray crystal structures of $[Co(sep)](S_2O_6){\cdot}H_2O$[5] and $[Co(\{(NH_3)_2sar\}](NO_3)_4{\cdot}H_2O$[39] which both exhibit trigonally twisted *lel*$_3$ conformations, it is likely that $[Co\{(NMe_3)_2sar\}]^{4+}$ also adopts this conformation in the solid state. In fact all high spin divalent metal ion complexes of hexadentate coordinated sar-type ligands exhibit this same *lel*$_3$ conformation in their crystal lattices.[39] Therefore, it would seem inevitable that the Co(II) ion in a high-spin condition would also require this trigonally twisted *lel*$_3$ conformation for this particular cage.

---

(37) Mason, S. F. *Quart. R. Chem. Soc.* **1963**, *17*, 20−66. Dubicki, L.; Ferguson, J.; Geue, R. J.; Sargeson, A. M. *Chem. Phys. Lett.* **1980**, *74*, 393−397.

(38) Lay, P. A.; Sargeson, A. M. *Inorg. Chem.* **1990**, *29*, 2762−2770.

(39) Comba, P.; Sargeson, A. M.; Engelhardt, L. M.; Harrowfield, J. MacB.; White, A. H.; Horn, E.; Snow, M. R. *Inorg. Chem.* **1985**, *24*, 2325−2327. Engelhardt, L. M.; White, A. H. Unpublished results.

Redox Chemistry. The substituents of $[Co\{(NMe_3)_2sar\}]^{5+/4+}$ make the redox potential, determined by cyclic voltammetry, much more positive than those of the $[Co(sep)]^{3+/2+}$ and $[Co(sar)]^{3+/2+}$ couples (Table 7). This is not surprising given the difference in charge and inductive effect of the positively charged substituent, and both effects make the Co(III) complex more susceptible to reduction. The apparently surprising results in Table 7 are that the redox potentials of the *ob*$_3$-$[Co\{(NMe_3)_2sar\}]^{5+}$ and *ob*$_3$-$[Co\{(NH_3)_2Me_3sar\}]^{5+}$ ions are so different; the former being ~250 mV more positive of that for the latter when superficially they might have been expected to be rather similar. Also the similarity between the redox potentials, measured the same way, from *ob*$_3$-$[Co\{(NMe_3)_2sar\}]^{5+}$ and mainly *lel* $[Co\{(NH_3)_2sar\}]^{5+}$ ions is surprising. The discrepancies arise from several factors. The $[Co\{(NMe_3)_2sar\}]^{5+}$ ion adopts the *ob*$_3$ conformation whereas the $[Co\{(NMe_3)_2sar\}]^{4+}$ ion would require the trigonally twisted *lel* conformation. The Taft polar substituent constants[40] require a substantial shift in potential for NMe_3^+ versus NH_3^+, which should result in the Co(III/II) redox potential of the hypothetical mainly *lel* $[Co\{(NMe_3)_2sar\}]^{5+}$/*lel*$_3$-$[Co\{(NMe_3)_2sar\}]^{4+}$ couple being ~200 mV more positive of that observed for the mainly *lel* $[Co\{(NH_3)_2sar\}]^{5+/4+}$ couple. By contrast, the data in Table 7 show that the Co(III)/(II) redox potential of *lel*$_3$-*fac*-$[Co\{(NH_3)_2Me_3sar\}]^{5+/4+}$ is 320 mV more positive than that of *ob*$_3$-*fac*-$[Co\{(NH_3)_2Me_3sar\}]^{5+/4+}$.[22] Since, in the $[Co\{(NMe_3)_2sar\}]^{5+}$ couple, the Co(III) complex is *ob*$_3$ and the Co(II) component is presumably *lel*$_3$, the two effects largely cancel and the potential remains close to that of the $[Co\{(NH_3)_2sar\}]^{5+/4+}$ couple. Experiments are currently underway also with the *lel*$_3$ and *ob*$_3$ conformers of $[Co\{(NH_2)_2Me_3sar\}]^{3+/2+}$ to try to quantify the solvation energies of these couples using the strategy developed previously.[41-43] These experiments, combined with molecular mechanics calculations and experiments into the effects of permethylation of the amine substituents of the relatively rigid Me_3sar cage complexes, should enable the various factors to be delineated more precisely.

The rate constant of electron self-exchange for the $[Co\{(NMe_3)_2sar\}]^{5+/4+}$ couple is 2 orders of magnitude smaller than that of the *fac*-*ob*$_3$-$[Co\{(NH_3)_2Me_3sar\}]^{5+/4+}$ couple. Also, the electron self-exchange rate constants of 5+/4+ cobalt cage couples with mainly *lel* conformations, in both oxidation states, are found to be approximately 30-fold smaller than those of *ob*$_3$ cage complexes.[22] Therefore, the rate constant of electron self-exchange in the Co(III)/(II) couple of $[Co\{(NMe_3)_2sar\}]^{5+/4+}$ cannot be explained if both ions of the couple adopt the *ob*$_3$ conformation in solution. From the arguments that have been outlined in the previous sections, it is likely that the Co(II) complex adopts a trigonally twisted *lel*$_3$ conformation, and therefore, the unusually slow rate can be explained in terms of a coupled conformational change with the electron transfer event.

Conclusions

In summary, this paper describes the synthesis and stereochemistry of new and interesting redox reagents albeit with a relative small electron self-exchange rate constant and high charges. The data collected with these complexes and related systems from NMR, electronic absorption, and CD spectroscopy, along with structural studies, have helped assign the solution conformations of numerous Co(III) cage complexes in aqueous solution.

Acknowledgment. We are grateful to the Australian Research Council and the National Science Foundation (J.R.P., Grant Nos. CHE 89-21985 and INT 90-15101) for financial support, the ANU Microanalytical Service and NMR center, Dr A. Arnold for the potentiometric titration data and D. Bogsanyi for technical assistance.

Supplementary Material Available: Tables of hydrogen atom positional parameters, anisotropic thermal parameters, torsion angles, and intermolecular hydrogen bonds (7 pages). Ordering information is given on any current masthead page.

---

(40) Ehrensen, S.; Brownlee, R. T. C.; Taft, R. W. *Prog. Phys. Org. Chem.* **1973**, *10*, 1-80.

(41) Lay, P. A.; McAlpine, N. S.; Hupp, J. T.; Weaver, M. J.; Sargeson, A. M. *Inorg. Chem.* **1990**, *29*, 4322-4328.

(42) Dubinska, K. B.; Lay, P. A.; McAlpine, N. S.; Gahan, L. R. In *Proceedings of the Seventh Australian Electrochemical Conference (Current and Potential Applications)*; Tran, T., Skyllas-Kazacos, M., Eds.; Royal Australian Chemical Institute: Sydney, Australia, 1988; pp 229-232.

(43) Lay, P. A. *J. Phys. Chem.* **1986**, *90*, 878-885.